THE JOURNAL OF PHYSICAL CHEMISTRY C

Article

pubs.acs.org/JPCC

Bipolar Electrochemistry with Organic Single Crystals for Wireless Synthesis of Metal–Organic Janus Objects and Asymmetric Photovoltage Generation

Iuliia Malytska,[†] Cécile Mézière,[‡] Marcin Kielar,[§] Lionel Hirsch,[§] Guillaume Wantz,[§] Narcis Avarvari,[‡] Alexander Kuhn,*[,†] and Laurent Bouffier*[,†]

[†]Univ. Bordeaux, ISM, CNRS, UMR 5255, Bordeaux INP, F-33400 Talence, France

[‡]CNRS, Laboratoire Moltech-Anjou, UMR 6200, Université d'Angers, 49045 Angers, France

[§]Univ. Bordeaux, IMS, CNRS, UMR 5218, Bordeaux INP, F-33405 Talence, France

ABSTRACT: Bipolar electrochemistry has recently emerged as a very unique method to address conducting particles in a wireless manner. The technique is often applied to the fabrication of Janus particles; however the chemical nature of the bipolar electrode has been essentially limited to carbon- or metal-based materials. Here, we report for the first time the use of conducting organic single crystals as bipolar electrodes for the preparation of a new generation of Janus objects. Fabre and Bechgaard salts involving respectively tetrathia- and tetraselenafulvalene were selected for proof-of-concept experiments. Such an approach allows to preserve the integrity of these fragile substrates because it necessitates neither electronic wiring nor mechanical contact. The site-selective electrodeposition of copper is successfully achieved, leading thus to a new metal–organic Janus structure. Subsequently, asymmetric generation of photovoltage under illumination is achieved due to the anisotropic presence of copper, making this approach interesting for the design of novel hybrid objects with applications in organic electronics or photocatalysis.

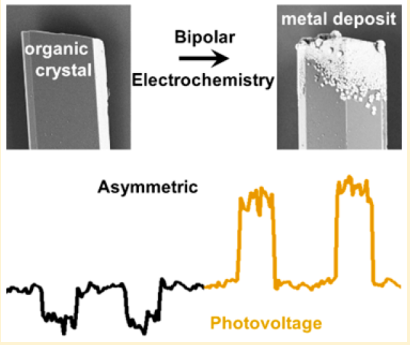

INTRODUCTION

Janus particles are the focus of major ongoing research studies because this class of asymmetric materials exhibits unprecedented anisotropic properties with many possible applications, especially for electronics, advanced spectroscopy, and optics. Several synthetic approaches have been proposed for the preparation of Janus objects whose common feature being indeed the necessity to break the symmetry of a chemical system.[1−7]

Among the various fabrication methods reported so far, bipolar electrochemistry (BPE) has recently emerged as a very unique approach.[8−11] BPE is already known for several decades and has been particularly used in the context of electrolysis and corrosion science.[12−16] In recent years, however, BPE has been reinvestigated and is nowadays a very hot topic with a much broader range of applications, especially in materials science and analytical chemistry.[17−24] BPE is an unconventional approach compared to a classic electrochemical setup where the electrochemical reactions take place at the surface of two different electrodes, namely the working and auxiliary electrode both connected to a potentiostat. In the case of BPE, an electric field is applied across an electrolyte solution where a conducting object is immersed and behaves as a floating electrode. The driving force is therefore the polarization potential established between the solution and the object, allowing thus to promote oxidation and reduction reactions at the opposite poles of the same object (Figure 1). BPE can be considered as an electrochemical break of symmetry of the corresponding bipolar electrode which behaves simultaneously as an anode and a cathode. Also, the bipolar electrode is

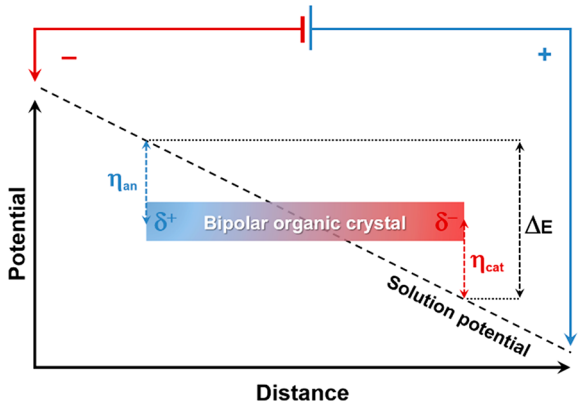

Figure 1. Schematic illustration of the principle of bipolar electrochemistry based on the polarization potential established alongside a conducting object immersed in an electrolyte and exposed to an electric field. In the present contribution, the bipolar electrode is an organic single crystal.

Received: March 21, 2017
Revised: May 20, 2017
Published: May 22, 2017

DOI: 10.1021/acs.jpcc.7b02678
J. Phys. Chem. C 2017, 121, 12921−12927

addressed electrochemically in a wireless fashion because there is no direct connection with the power supply. Finally, one of the key advantages of BPE is that it does not directly involve a 2-dimensional interface to break the symmetry, providing a powerful tool for the bulk (i.e., 3D) fabrication or activation of Janus objects.[25,26] It is also noteworthy that BPE can be used to generate surface anisotropy based on the gradient of polarization potential alongside the bipolar electrode. This has been exemplified by several contributions showing the variation of chemical composition, morphology, or thickness and therefore of the resulting physical, optical, or spectroscopic properties.[27−37]

So far, BPE has proven to be very versatile for site-selective wireless electrodeposition by tuning the nature of the chemical species involved in the bipolar reactions at the extremities of a conducting object. For instance, the reduction of a metal precursor to form the corresponding metal,[38−40] the electrooxidation of a monomer to form a polymer layer,[41] the electrografting of an organic layer,[42] pH-induced local precipitation,[43] and the deposition of various inorganic structures were reported.[44,45] However, all these experiments were performed on bipolar electrodes made out of either metal or carbon allotropes, thus exhibiting a high electrical conductivity.[46−48] The reason is obviously because BPE is favored when the bipolar electrode is more conductive than the surrounding media due to the competition between the Faradaic current flowing through the bipolar electrode and the ionic current occurring across the electrolyte. As a matter of fact, varying the chemical nature of the bipolar electrode has not been widely investigated even if BPE experiments with other inorganic bipolar electrodes such as tin-doped indium oxide (ITO) surfaces or TiO_2 tubes were reported.[49] It is also noteworthy that organic thin layers based on conductive polymers were reported to behave as bipolar surfaces.[28,30,32]

In order to extend the application range of Janus particles prepared by BPE, we report in the present contribution for the first time the use of organic single crystals as bipolar electrodes. We selected Fabre and Bechgaard salts, which are well-known organic conductor structures based on tetramethyltetrathiafulvalene (TMTTF) and tetramethyltetraselenafulvalene (TMTSF) as donors (Scheme 1) and hexafluorophosphate as counterion.[50] These materials have been identified as possible bipolar electrode candidates because they exhibit a suitable conductivity and have also interesting potential applications in organic electronics or photocatalysis. It is also noteworthy that such organic crystals need to be handled carefully because they are relatively fragile and can therefore be irreversibly damaged during conventional electrodeposition experiments. Here, the key advantage of BPE is indeed the possibility to modify such crystals without any electronic or mechanical contact.

Scheme 1. Chemical Structure of Tetramethyltetrathiafulvalene (TMTTF) and Tetramethyltetraselenafulvalene (TMTSF)

TMTTF TMTSF

MATERIALS AND METHODS

Chemicals. $(TMTTF)_2PF_6$ and $(TMTSF)_2PF_6$ crystals used in this study were classically prepared by electrocrystallization as described in the literature.[51,52]

All aqueous solutions were prepared with Milli-Q grade water (Millipore, resistivity 18.2 MΩ cm at 25 °C). Copper sulfate ($CuSO_4$, anhydrous, 98% purity) was purchased from Alfa Aesar. Hydroquinone (HOC_6H_4OH, abbreviated H_2Q, 99.5% minimal purity) was purchased from Sigma-Aldrich. Dichloromethane (CH_2Cl_2, chromasolv, ≥99.8%) and tetrabutylammonium hexafluorophosphate (Bu_4NPF_6, for electrochemical analysis, ≥99.0%) were purchased from Sigma-Aldrich (supplier, grade). Tetramethyltetraselenafulvalene (TMTSF, 97%) was purchased from Acros Organics.

Bipolar Electrochemistry. Bipolar electrodeposition experiments were performed in a homemade cell comprising two plastic cuvettes connected by a glass capillary. The studied organic crystals were positioned inside the capillary prior to BPE experiments. The feeder electrodes are gold plates (10 × 25 mm) purchased from ACM (78640 Villiers, France). The typical distance between both feeder electrodes is ∼50 mm, and they are connected to an external power supply (Keithley 6517 electrometer).

Microscopy. Organic crystals were characterized by using an optical stereomacroscope (Leica MSV266) and a scanning electron microscope (Hitachi, TM-1000).

Cyclic Voltammetry. Cyclic voltammetry (CV) experiments were carried out in a conventional electrochemical cell comprising a gold working electrode (ϕ = 2.0 mm), a platinum mesh counter electrode, and a silver wire pseudoreference connected to a potentiostat (Autolab, PGSTAT12). The working electrode was carefully polished with alumina and rinsed before each experiment, and the CVs were recorded in CH_2Cl_2 containing 1 mM TMTTF and 0.1 M Bu_4NPF_6 at room temperature. CVs were measured at different scan rates ranging from 0.01 to 1.00 V s^{-1}.

Photovoltage Measurements. Photovoltage measurements were performed with two carbon Scotch tape electrodes (SPI Supplies, 8 mm width) with ∼1 mm spacing and connected to a high-precision voltmeter (Keithley 2001 multimeter). A LabVIEW script (version 9.0) was written and used to record the photovoltage signal. Organic crystals were carefully positioned between both electrodes prior to measurements. A commercial red laser beam (λ = 635 nm) was used for the illumination of the extremities of these crystals.

RESULTS AND DISCUSSION

$(TMTTF)_2PF_6$ and $(TMTSF)_2PF_6$ were prepared by a classic electrocrystallization method, and the average length of these crystals is in the range of 1−3 mm and a typical diameter up to ∼200 μm.[52,53] The characteristic conductivity of these Bechgaard crystal phases is of the order of 20 S cm^{-1} for the first one (TMTTF) and 500 S cm^{-1} for the second one (TMTSF) at room temperature with metallic behavior.[52−54] Therefore, their intrinsic conductivity is at least 3 orders of magnitude larger than the typical ionic conductivity of the supporting electrolyte (∼ mS cm^{-1}).

As proof-of-principle to demonstrate the possibility to use such organic crystals as bipolar electrodes, the site-selective electrodeposition of copper was chosen. Indeed, this metal has already been used at several occasions for BPE experi-

DOI: 10.1021/acs.jpcc.7b02678
J. Phys. Chem. C 2017, 121, 12921−12927

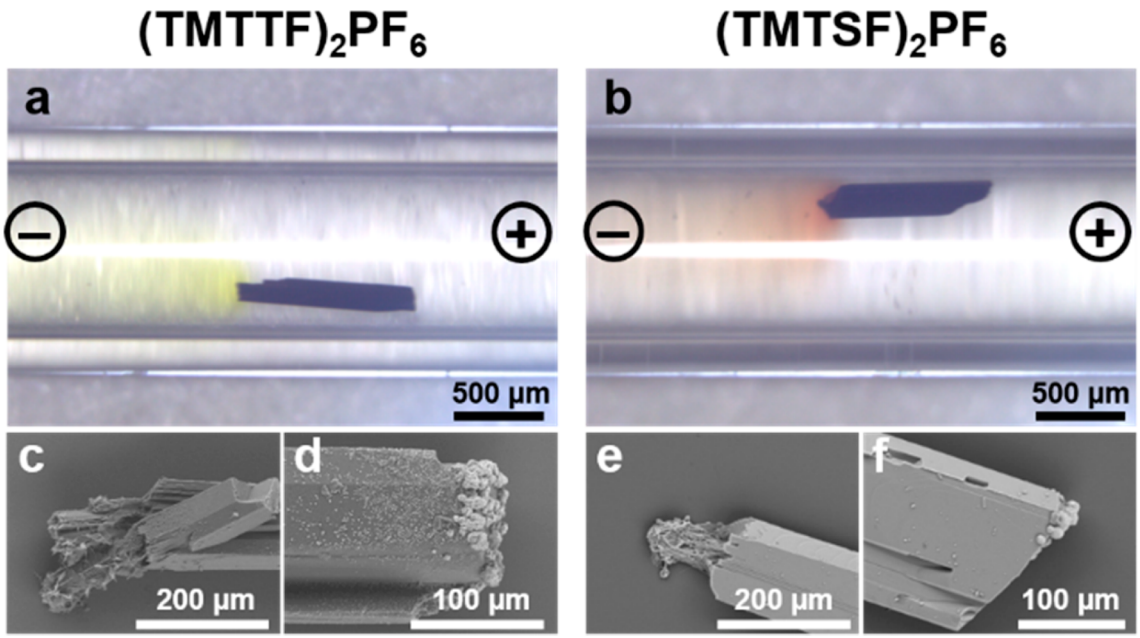

Figure 2. Bipolar electrodeposition experiments performed on organic crystals. Optical image of an organic crystal of $(TMTTF)_2PF_6$ positioned inside a glass capillary filled with 10 mM $CuSO_4$ aqueous solution and exposed to an electric field of 5 V cm^{-1}. The polarization of both feeder electrodes is indicated (a). Idem with a crystal of $(TMTSF)_2PF_6$ and an electric field of 6.5 V cm^{-1} (b). Scanning electron micrographs of the left (c) and right (d) extremities of $(TMTTF)_2PF_6$ organic crystals damaged at the anode side and modified with copper at the cathode side. Idem in the case of $(TMTSF)_2PF_6$ (e and f, respectively).

ments.[36,46,55] The electrochemical reactions that need to be coupled across the bipolar electrode are therefore cupric ion reduction at the cathode side (eq 1) and water oxidation at the anodic pole (eq 2):

$$Cu^{2+} + 2e^- \rightarrow Cu^0 \quad (E_1^\circ = 0.34 \text{ V vs NHE}) \tag{1}$$

$$2H_2O \rightarrow O_2 + 4H^+ \rightarrow 4e^- \quad (E_2^\circ = 1.23 \text{ V vs NHE}) \tag{2}$$

It means that in order to achieve BPE-induced copper deposition, the minimal polarization potential difference between the two poles of the bipolar electrode should be 1.23 V − 0.34 V = 0.89 V. BPE experiments were conducted in an electrochemical cell built with two reservoirs, linked together by a glass capillary, each side containing a gold feeder electrode connected to an external power supply. The organic crystal is positioned in the capillary, and the whole cell is filled with a 10 mM aqueous solution of $CuSO_4$. The applied electric field should be at least 8.9 V cm^{-1} if considering a 1 mm long crystal. Also, the distance between both feeder electrodes was fixed at 5 cm, meaning that under these experimental conditions a potential of at least ∼45 V should be imposed by the external power supply in order to achieve the necessary electric field strength.

Bipolar electrodeposition was conducted on both $(TMTTF)_2PF_6$ and $(TMTSF)_2PF_6$ crystals, and the corresponding experiments were monitored in situ by optical microscopy while applying the electric field (Figures 2a and 2b).

From these representative optical images, one can easily identify the organic crystal positioned inside the capillary and also a marked coloration of the solution in yellow for TMTTF (Figure 2a) and in red for TMTSF (Figure 2b) with a maximum intensity located at the left side of the bipolar electrode, being actually the anodic pole. These colored compounds seem to migrate towards the feeder cathode, revealing that they are indeed positively charged molecules. Both sides of the crystals were also characterized by scanning electron microscopy (SEM) as shown in Figures 2c–f. These images show that the electrodeposition of Cu as discrete clusters (size <10 μm) does occur at the cathodic extremity of both crystals (Figures 2d and 2f). On the other hand, the anodic pole of the crystal was clearly damaged during BPE, and the corresponding images show an extended portion of the crystals where electro-induced dissolution seems to take place (Figures 2c and 2e). Therefore, an oxidative degradation of both TMTTF- and TMTSF-based crystals was observed under BPE conditions, encouraging us to further investigate the electrochemical characterization of these two donors. It is noteworthy that absolutely no degradation was observed without applying the electric field, meaning that both crystals are electrochemically stable at open-circuit potential.

The electrochemical behavior of the donor moieties was studied by cyclic voltammetry (CV) recorded in an aprotic organic solvent because of their low solubility in water. Both CV experiments were comparable, and a typical CV recorded at several scan rates is presented in Figure 3. These data were obtained from a 1 mM TMTSF solution in CH_2Cl_2 containing 0.1 M Bu_4NPF_6 as supporting electrolyte.

The cyclic voltammogram features two well-defined reversible processes corresponding to two stepwise monoelectronic oxidations of the tetraselenafulvalene moiety. The first oxidation is centered at 0.36 V versus a silver pseudoreference and corresponds to the removal of an electron from TMTSF to form a radical cation, whereas the second one occurs at 0.83 V and is assigned to the formation of a dication:

$$TMTSF \rightarrow TMTSF^{\bullet+} + e^- \quad (E_3^\circ \sim 0.56 \text{ V vs NHE}) \tag{3}$$

DOI: 10.1021/acs.jpcc.7b02678
J. Phys. Chem. C 2017, 121, 12921−12927

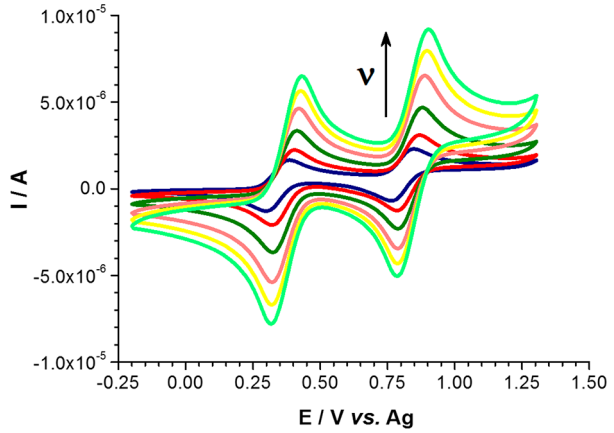

Figure 3. Cyclic voltammograms of 1 mM TMTSF in CH_2Cl_2 with 0.1 M Bu_4NPF_6 as supporting electrolyte recorded with a gold working electrode at various scan rates (ν = 0.05, 0.10, 0.250, 0.50, 0.75, and 1.00 V s^{-1}, respectively). The counter electrode was a platinum mesh, and a silver wire was used as pseudoreference.

$$TMTSF^{\bullet+} \rightarrow TMTSF^{2+} + e^- \quad (E_4^\circ \sim 1.03\ V\ vs\ NHE) \tag{4}$$

These values are consistent with previously reported data (0.33 and 0.70 V versus SCE for TMTTF in CH_3CN).[56] Even if the BPE experiments were performed in aqueous phase with the Bechgaard salts, whereas the electrochemical characterization of the donors was carried out in an organic solvent, it is clear that TMTTF and TMTSF are much easier to oxidize than water. This is why our first set of BPE tests led to a degradation of these organic crystals (Figure 2). Indeed, the reduction of Cu^{2+} at the cathodic pole is coupled with the oxidation of the crystal at the anodic side. It is also noteworthy that the changes in color observed with optical microscopy (Figure 2a,b) are attributed to the electro-oxidation of $TMTTF^{0/+}$ or $TMTSF^{0/+}$ into the corresponding dications as already observed for example with TTF by in situ visible absorption spectroelectrochemistry.[57]

On the basis of these new data, another set of BPE experiments was carried out by adding to the electrolyte a sacrificial coreactant which is easier to oxidize than the donor in the organic crystal. Here, it is important to remind that the donor molecules in the crystal structures are overlapping symmetrically giving rise to a formally 1/2 filled band in the dimerized situation. For that purpose, hydroquinone (H_2Q) was selected because it exhibits appropriate redox properties with a formal oxidation potential less positive than the oxidation of the fulvalene donor into the dicationic forms $TMTTF^{2+}$ or $TMTSF^{2+}$, respectively:

$$H_2Q \rightarrow Q + 2H^{2+} + 2e^- \quad (E_5^\circ \sim 0.70\ V\ vs\ NHE) \tag{5}$$

As a consequence, the two redox half-reactions involved in the BPE electrodeposition will become the ones reported in eqs 1 and 5, and therefore the necessary electric field will be much lower than previously.

Therefore, a new series of BPE tests was conducted by applying an electric field typically lower than 3−4 V cm^{-1}, and the corresponding modified crystals (length ≥1 mm) were characterized by SEM imaging (Figure 4).

As one can see in the corresponding micrographs, such an approach which takes advantage of a sacrificial redox coreactant was successful. The cathodic edge was indeed correctly modified with copper (Figures 4b and 4d) while the anodic side remained undamaged (Figures 4a and 4c). In the latter cases, an electric field of 2.6 V cm^{-1} was applied and resulted in a metal deposit that is well-focused at the very edge of the organic crystals. A large number of asymmetric objects of various lengths were prepared according to the same procedure, and as expected, a longer deposition zone was observed when using the longest crystals (2.5−3 mm) such as the one shown in Figure 5a. These long single crystals were then selected for further electrical characterization as they are easier to handle.

Photovoltage measurements were recorded to demonstrate the influence of the localized deposit on the physical properties of the newly prepared metal/organic hybrid material. To do so, a very simple experimental setup was chosen where the organic crystal is positioned between two carbon-tape stripes connected to a voltmeter (Figure 5b). The open-circuit voltage was then measured while illuminating either one side or the other of the asymmetric materials with a red laser (λ = 650 nm). A representative time evolution of the photovoltage generated across a modified $(TMTSF)_2PF_6$ crystal as a function of the light excitation is shown in Figure 5c. Here, the geometry of the device is similar to a metal/semiconductor/metal (MSM) photodetector architecture. It means that in this configuration two metal/semiconductor Schottky contacts are positioned in front of each other, and therefore the photovoltage polarity depends on the illumination side.[58] Indeed, the intensity of the photovoltage was found to be asymmetric with a different amplitude depending on whether the excitation was focused on the modified versus nonmodified side of the crystal. This is assigned to the different nature of the contact (and corresponding work functions) between the right and left sides with or without the presence of copper. A control experiment was also recorded with a pristine crystal. In this

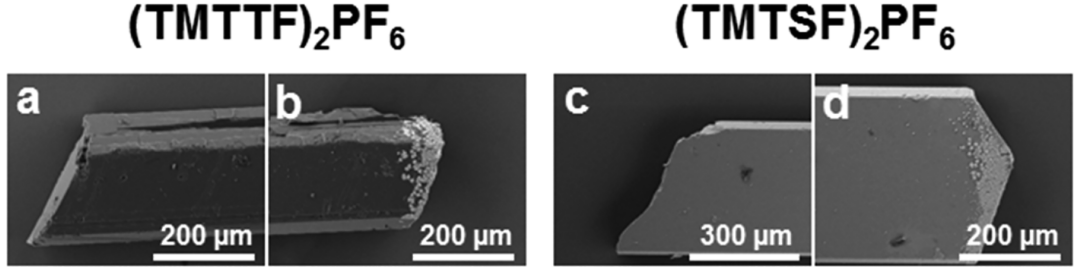

Figure 4. Scanning electron micrographs of the left (a) and right (b) extremities of a $(TMTTF)_2PF_6$ organic crystal where the anode side remains intact (due to the addition of hydroquinone as a sacrificial coreactant), whereas the cathode side is modified with copper. Idem in the case of $(TMTSF)_2PF_6$ (c and d, respectively).

DOI: 10.1021/acs.jpcc.7b02678
J. Phys. Chem. C 2017, 121, 12921−12927

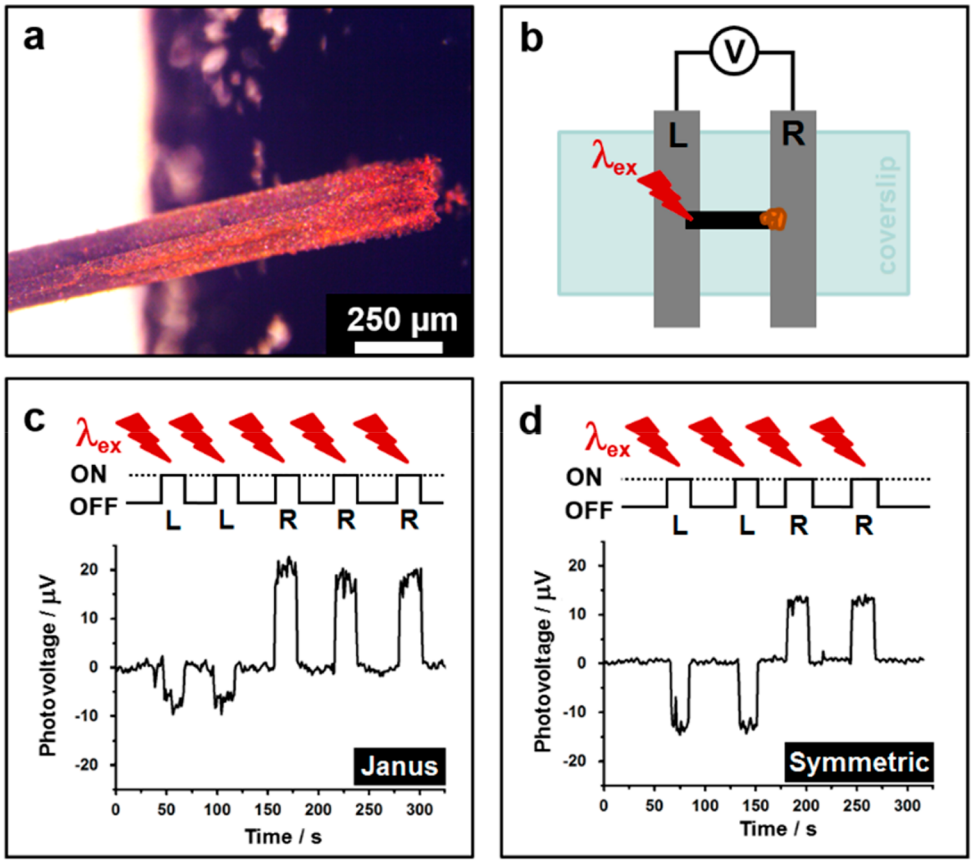

Figure 5. Optical image of the Janus $(TMTSF)_2PF_6$ crystal modified at one extremity with copper (a). Illustration of the experimental photovoltage setup with the organic crystal bridging two carbon electrodes connected to a voltmeter. The excitation source is a red laser directed alternatively on the left (L) and right (R) side of the electrode/crystal contact (b). Sequence of illumination and corresponding photovoltage recorded with a Janus (c) and unmodified (i.e., symmetric) organic crystal (d), respectively.

latter case, the absolute intensity of the photovoltage was found to be independent of the excitation side, confirming the symmetry breaking assigned to the Cu deposit (Figure 5d). Such an asymmetric photovoltage behavior was reported recently in the case of Janus graphene sheets[59] and is observed here for the first time on a more complex Janus organic single crystal conductor. Finally, the comparison between a modified and an unmodified crystal confirms also that the chemical integrity of the Bechgaard salt was not altered by the copper electrodeposition process.

CONCLUSIONS

Using BPE has already proven to be successful for the fabrication of various asymmetric Janus particles. So far, the almost unique strategy was based on the site-selective electrodeposition of a redox-active precursor at one extremity of either carbon or metal bipolar electrodes. The choice of these substrates is straightforward because they are indeed very good conductors typically used as electrode materials for conventional electrochemistry. In an effort to extend the scope and potentialities of BPE, Fabre and Bechgaard salts based on TMTTF and TMTSF moieties were selected and used as bipolar electrodes. This is the first demonstration of the use of organic crystal conductors in bipolar electrochemistry for which copper metal electrodeposition was chosen. The approach opens the route to new families of Janus particles that can be prepared by BPE in the bulk phase. The corresponding asymmetric objects were characterized by optical imaging and electron microscopy revealing that the edge of the crystal acting as an anode is very sensitive to electrodissolution. This drawback has been overcome by the addition of a sacrificial coreactant with an appropriate redox potential in order to carry out bipolar electrodeposition without altering the chemical structure of the crystal. Finally, asymmetric photovoltage generation could be observed as a result of the intrinsic break of symmetry provided by the site-selective metal deposition. We anticipate that this kind of new functional hybrid materials will readily be employed for applications in organic electronics and/or photocatalysis, especially for electronic display or photoactive electronic devices. Besides, more elaborated TTF-based conducting crystals with other functionalities will be considered as possible BPE organic electrodes.[60,61]

AUTHOR INFORMATION

Corresponding Authors

*E-mail: alexander.kuhn@enscbp.fr (A.K.).
*E-mail: laurent.bouffier@enscbp.fr (L.B.).

ORCID

Laurent Bouffier: 0000-0002-0346-1254

Notes

The authors declare no competing financial interest.

ACKNOWLEDGMENTS

I.M. is grateful for financial support provided by the University of Bochum in the frame of the European project Bioenergy

DOI: 10.1021/acs.jpcc.7b02678
J. Phys. Chem. C 2017, 121, 12921−12927

(FP7-PEOPLE-2013-ITN 607793). Financial support from the RFI LUMOMAT (Région Pays de la Loire) is also acknowledged.

■ ABBREVIATIONS

BPE, bipolar electrochemistry; ITO, tin-doped indium oxide; TMTTF, tetramethyltetrathiafulvalene; TMTSF, tetramethyltetraselenafulvalene; SEM, scanning electron microscopy; CV, cyclic voltammetry; H_2Q, hydroquinone; MSM, metal/semiconductor/metal.

■ REFERENCES

(1) Perro, A.; Reculusa, S.; Ravaine, S.; Bourgeat-Lami, E.; Duguet, E. Design and Synthesis of Janus Micro- and Nanoparticles. *J. Mater. Chem.* **2005**, *15*, 3745−3760.
(2) Walther, A.; Muller, A. H. E. Janus Particles. *Soft Matter* **2008**, *4*, 663−668.
(3) Jiang, S.; Chen, Q.; Tripathy, M.; Luijten, E.; Schweizer, K. S.; Granick, S. Janus Particle Synthesis and Assembly. *Adv. Mater.* **2010**, *22*, 1060−1071.
(4) Hu, J.; Zhou, S.; Sun, Y.; Fang, X.; Wu, L. Fabrication, Properties and Applications of Janus Particles. *Chem. Soc. Rev.* **2012**, *41*, 4356−4378.
(5) Loget, G.; Kuhn, A. Bulk Synthesis of Janus Objects and Asymmetric Patchy Particles. *J. Mater. Chem.* **2012**, *22*, 15457−15474.
(6) Walther, A.; Müller, A. H. Janus Particles: Synthesis, Self-Assembly, Physical Properties, and Applications. *Chem. Rev.* **2013**, *113*, 5194−5261.
(7) Liang, F.; Zhang, C.; Yang, Z. Rational Design and Synthesis of Janus Composites. *Adv. Mater.* **2014**, *26*, 6944−6949.
(8) Fosdick, S. E.; Knust, K. N.; Scida, K.; Crooks, R. M. Bipolar Electrochemistry. *Angew. Chem. Int. Ed.* **2013**, *52*, 10438−10456.
(9) Loget, G.; Zigah, D.; Bouffier, L.; Sojic, N.; Kuhn, A. Bipolar Electrochemistry: From Materials Science to Motion and Beyond. *Acc. Chem. Res.* **2013**, *46*, 2513−2523.
(10) Sequeira, C. A. C.; Cardoso, D. S. P.; Gameiro, M. L. F. Bipolar Electrochemistry, a Focal Point of Future Research. *Chem. Eng. Commun.* **2016**, *203*, 1001−1008.
(11) Inagi, S. Fabrication of Gradient Polymer Surfaces Using Bipolar Electrochemistry. *Polym. J.* **2016**, *48*, 39−44.
(12) Eardley, D. C.; Handley, D.; Andrew, S. P. S. Bipolar Electrolysis with Intra Phase Conduction in Two Phase Media. *Electrochim. Acta* **1973**, *18*, 839−848.
(13) Fleischmann, M.; Ghoroghchian, J.; Rolison, D.; Pons, S. Electrochemical Behavior of Dispersions of Spherical Ultramicroelectrodes. *J. Phys. Chem.* **1986**, *90*, 6392−6400.
(14) Duval, J.; Kleijn, J. M.; van Leeuwen, H. P. Bipolar Electrode Behaviour of the Aluminium Surface in a Lateral Electric Field. *J. Electroanal. Chem.* **2001**, *505*, 1−11.
(15) Munktell, S.; Tydén, M.; Högström, J.; Nyholm, L.; Björefors, F. Bipolar Electrochemistry for High-Throughput Corrosion Screening. *Electrochem. Commun.* **2013**, *34*, 274−277.
(16) Munktell, S.; Nyholm, L.; Björefors, F. Towards High Throughput Corrosion Screening Using Arrays of Bipolar Electrodes. *J. Electroanal. Chem.* **2015**, *747*, 77−82.
(17) Bradley, J.-C.; Chen, H.-M.; Crawford, J.; Eckert, J.; Ernazarova, K.; Kurzeja, T.; Lin, M.; McGee, M.; Nadler, W.; Stephens, S. G. Creating Electrical Contacts Between Metal Particles Using Directed Electrochemical Growth. *Nature* **1997**, *389*, 268−271.
(18) Bradley, J. C.; Ma, Z. Contactless Electrodeposition of Palladium Catalysts. *Angew. Chem. Int. Ed.* **1999**, *38*, 1663−1666.
(19) Mavré, F.; Anand, R. K.; Laws, D. R.; Chow, K.-F.; Chang, B.-Y.; Crooks, J. A.; Crooks, R. M. Bipolar Electrodes: a Useful Tool for Concentration, Separation, and Detection of Analytes in Microelectrochemical Systems. *Anal. Chem.* **2010**, *82*, 8766−8774.
(20) Wu, M.-S.; Qian, G.-s.; Xu, J.-J.; Chen, H.-Y. Sensitive Electrochemiluminescence Detection of c-Myc mRNA in Breast Cancer Cells on a Wireless Bipolar Electrode. *Anal. Chem.* **2012**, *84*, 5407−5414.
(21) Zhang, X.; Chen, C.; Li, J.; Zhang, L.; Wang, E. New Insight into a Microfluidic-Based Bipolar System for an Electrochemiluminescence Sensing Platform. *Anal. Chem.* **2013**, *85*, 5335−5339.
(22) Bouffier, L.; Ravaine, V.; Sojic, N.; Kuhn, A. Electric Fields for Generating Unconventional Motion of Small Objects. *Curr. Opin. Colloid Interface Sci.* **2016**, *21*, 57−64.
(23) Allagui, A.; Abdelkareem, M. A.; Alawadhi, H.; Elwakil, A. S. Reduced Graphene Oxide Thin Film on Conductive Substrates by Bipolar Electrochemistry. *Sci. Rep.* **2016**, *6*, 21282.
(24) Koizumi, Y.; Shida, N.; Ohira, M.; Nishiyama, H.; Tomita, I.; Inagi, S. Electropolymerization on Wireless Electrodes Towards Conducting Polymer Microfibre Networks. *Nat. Commun.* **2016**, *7*, 10404.
(25) Loget, G.; Roche, J.; Kuhn, A. True Bulk Synthesis of Janus Objects by Bipolar Electrochemistry. *Adv. Mater.* **2012**, *24*, 5111−5116.
(26) Sentic, M.; Arbault, S.; Bouffier, L.; Manojlovic, D.; Kuhn, A.; Sojic, N. 3D Electrogenerated Chemiluminescence: From Surface-Confined Reactions to Bulk Emission. *Chem. Sci.* **2015**, *6*, 4433−4437.
(27) Ulrich, C.; Andersson, O.; Nyholm, L.; Björefors, F. Formation of Molecular Gradients on Bipolar Electrodes. *Angew. Chem. Int. Ed.* **2008**, *47*, 3034−3036.
(28) Inagi, S.; Ishiguro, Y.; Atobe, M.; Fuchigami, T. Bipolar Patterning of Conducting Polymers by Electrochemical Doping and Reaction. *Angew. Chem. Int. Ed.* **2010**, *49*, 10136−10139.
(29) Ramakrishnan, S.; Shannon, C. Display of Solid-State Materials Using Bipolar Electrochemistry. *Langmuir* **2010**, *26*, 4602−4606.
(30) Ishiguro, Y.; Inagi, S.; Fuchigami, T. Gradient Doping of Conducting Polymer Films by Means of Bipolar Electrochemistry. *Langmuir* **2011**, *27*, 7158−7162.
(31) Ramaswamy, R.; Shannon, C. Screening the Optical Properties of Ag−Au Alloy Gradients Formed by Bipolar Electrodeposition Using Surface Enhanced Raman Spectroscopy. *Langmuir* **2011**, *27*, 878−881.
(32) Ishiguro, Y.; Inagi, S.; Fuchigami, T. Site-Controlled Application of Electric Potential on a Conducting Polymer "Canvas". *J. Am. Chem. Soc.* **2012**, *134*, 4034−4036.
(33) Loget, G.; So, S.; Hahn, R.; Schmuki, P. Bipolar Anodization Enables the Fabrication of Controlled Arrays of TiO_2 Nanotube Gradients. *J. Mater. Chem. A* **2014**, *2*, 17740−17745.
(34) Zhang, J.; Meng, Y.; Yu, X. Control of Friction Distribution on Stainless Steel Surface in Sodium Dodecyl Sulfate Aqueous Solution by Bipolar Electrochemistry. *Tribol. Lett.* **2015**, *59*, 43.
(35) Tisserant, G.; Fattah, Z.; Ayela, C.; Roche, J.; Plano, B.; Zigah, D.; Goudeau, B.; Kuhn, A.; Bouffier, L. Generation of Metal Composition Gradients by Means of Bipolar Electrodeposition. *Electrochim. Acta* **2015**, *179*, 276−281.
(36) Tisserant, G.; Gillion, J.; Lannelongue, J.; Fattah, Z.; Garrigue, P.; Roche, J.; Zigah, D.; Kuhn, A.; Bouffier, L. Single-Step Screening of the Potential Dependence of Metal Layer Morphologies Along Bipolar Electrodes. *ChemElectroChem.* **2016**, *3*, 387−391.
(37) Kayran, Y. U.; Eßmann, V.; Grützke, S.; Schuhmann, W. Selection of Highly SERS-Active Nanostructures from a Size Gradient of Au Nanovoids on a Single Bipolar Electrode. *ChemElectroChem.* **2016**, *3*, 399−403.
(38) Warakulwit, C.; Nguyen, T.; Majimel, J.; Delville, M.-H.; Lapeyre, V.; Garrigue, P.; Ravaine, V.; Limtrakul, J.; Kuhn, A. Dissymmetric Carbon Nanotubes by Bipolar Electrochemistry. *Nano Lett.* **2008**, *8*, 500−504.
(39) Roche, J.; Loget, G.; Zigah, D.; Fattah, Z.; Goudeau, B.; Arbault, S.; Bouffier, L.; Kuhn, A. Straight-Forward Synthesis of Ringed Particles. *Chem. Sci.* **2014**, *5*, 1961−1966.
(40) Allagui, A.; Salameh, T.; Alawadhi, H. Dendritic CuO Structures Synthesized by Bipolar Electrochemical Process for Electrochemical Energy Storage. *J. Electroanal. Chem.* **2015**, *750*, 107−113.
(41) Loget, G.; Lapeyre, V.; Garrigue, P.; Warakulwit, C.; Limtrakul, J.; Delville, M.-H.; Kuhn, A. Versatile Procedure for Synthesis of Janus-Type Carbon Tubes. *Chem. Mater.* **2011**, *23*, 2595−2599.

DOI: 10.1021/acs.jpcc.7b02678
J. Phys. Chem. C 2017, 121, 12921−12927

(42) Kumsapaya, C.; Bakaï, M. F.; Loget, G.; Goudeau, B.; Warakulwit, C.; Limtrakul, J.; Kuhn, A.; Zigah, D. Wireless Electrografting of Molecular Layers for Janus Particle Synthesis. *Chem. - Eur. J.* **2013**, *19*, 1577−1580.
(43) Loget, G.; Roche, J.; Gianessi, E.; Bouffier, L.; Kuhn, A. Indirect Bipolar Electrodeposition. *J. Am. Chem. Soc.* **2012**, *134*, 20033−20036.
(44) Fattah, Z.; Roche, J.; Garrigue, P.; Zigah, D.; Bouffier, L.; Kuhn, A. Chemiluminescence from Asymmetric Inorganic Surface Layers Generated by Bipolar Electrochemistry. *ChemPhysChem* **2013**, *14*, 2089−2093.
(45) Yadnum, S.; Roche, J.; Lebraud, E.; Négrier, P.; Garrigue, P.; Bradshaw, D.; Warakulwit, C.; Limtrakul, J.; Kuhn, A. Site-Selective Synthesis of Janus-type Metal-Organic Framework Composites. *Angew. Chem., Int. Ed.* **2014**, *53*, 4001−4005.
(46) Loget, G.; Larcade, G.; Lapeyre, V.; Garrigue, P.; Warakulwit, C.; Limtrakul, J.; Delville, M. H.; Ravaine, V.; Kuhn, A. Single Point Electrodeposition of Nickel for the Dissymmetric Decoration of Carbon Tubes. *Electrochim. Acta* **2010**, *55*, 8116−8120.
(47) Fattah, Z.; Loget, G.; Lapeyre, V.; Garrigue, P.; Warakulwit, C.; Limtrakul, J.; Bouffier, L.; Kuhn, A. Straightforward Single-Step Generation of Microswimmers by Bipolar Electrochemistry. *Electrochim. Acta* **2011**, *56*, 10562−10566.
(48) Koizumi, Y.; Shida, N.; Tomita, I.; Inagi, S. Bifunctional Modification of Conductive Particles by Iterative Bipolar Electrodeposition of Metals. *Chem. Lett.* **2014**, *43*, 1245−1247.
(49) Ongaro, M.; Roche, J.; Kuhn, A.; Ugo, P. Asymmetric Modification of TiO_2 Nanofibers with Gold by Electric-Field-Assisted Photochemistry. *ChemElectroChem.* **2014**, *1*, 2048−2051.
(50) Jacobsen, C. S.; Tanner, D. B.; Bechgaard, K. Optical and Infrared Properties of Tetramethyltetraselenafulvalene $[(TMTSF)_2X]$ and Tetramethyltetrathiafulvalene $[(TMTTF)_2X]$ Compounds. *Phys. Rev. B: Condens. Matter Mater. Phys.* **1983**, *28*, 7019−7032.
(51) Delhaes, P.; Coulon, C.; Amiell, J.; Flandrois, S.; Toreilles, E.; Fabre, J. M.; Giral, L. Physical Properties of One Dimensional Conductors. *Mol. Cryst. Liq. Cryst.* **1979**, *50*, 43−58.
(52) Bechgaard, K.; Jacobsen, C. S.; Mortensen, K.; Pedersen, H. J.; Thorup, N. The Properties of Five Highly Conducting Salts: $(TMTSF)_2X$, X = PF_6^-, AsF_6^-, SbF_6^-, BF_4^- and NO_3^-, Derived from Tetramethyltetraselenafulvalene (TMTSF). *Solid State Commun.* **1980**, *33*, 1119−1125.
(53) Moser, J.; Gabay, M.; Auban-Senzier, P.; Jérome, D.; Bechgaard, K.; Fabre, J. M. Transverse Transport in $(TM)_2X$ Organic Conductors: Possible Evidence for a Luttinger Liquid. *Eur. Phys. J. B* **1998**, *1*, 39−46.
(54) Nad, F.; Monceau, P.; Carcel, C.; Fabre, J. M. Dielectric Response of the Charge-Induced Correlated State in the Quasi-One-Dimensional Conductor $(TMTTF)_2PF_6$. *Phys. Rev. B: Condens. Matter Mater. Phys.* **2000**, *62*, 1753−1756.
(55) Fattah, Z.; Garrigue, P.; Lapeyre, V.; Kuhn, A.; Bouffier, L. Controlled Orientation of Asymmetric Copper Deposits on Carbon Microobjects by Bipolar Electrochemistry. *J. Phys. Chem. C* **2012**, *116*, 22021−22027.
(56) Coffen, D. L.; Chambers, J. Q.; Williams, D. R.; Garrett, P. E.; Canfield, N. D. Tetrathioethylenes. *J. Am. Chem. Soc.* **1971**, *93*, 2258−2268.
(57) Huchet, L.; Akoudad, S.; Levillain, E.; Roncali, J.; Emge, A.; Bäuerle, P. Spectroelectrochemistry of Electrogenerated Tetrathiafulvalene-Derivatized Poly(thiophenes): Toward a Rational Design of Organic Conductors with Mixed Conduction. *J. Phys. Chem. B* **1998**, *102*, 7776−7781.
(58) Hirsch, L.; Moretto, P.; Duboz, J. Y.; Reverchon, J. L.; Damilano, B.; Grandjean, N.; Semond, F.; Massies, J. Field Distribution and Collection Efficiency in an AlGaN Metal−Semiconductor−Metal Detector. *J. Appl. Phys.* **2002**, *91*, 6095−6098.
(59) Zuccaro, L.; Kuhn, A.; Konuma, M.; Yu, H. K.; Kern, K.; Balasubramanian, K. Selective Functionalization of Graphene Peripheries by using Bipolar Electrochemistry. *ChemElectroChem.* **2016**, *3*, 372−377.
(60) Pop, F.; Auban-Senzier, P.; Frąckowiak, A.; Ptaszyński, K.; Olejniczak, I.; Wallis, J. D.; Canadell, E.; Avarvari, N. Chirality Driven Metallic versus Semiconducting Behavior in a Complete Series of Radical Cation Salts Based on Dimethyl-Ethylenedithio-Tetrathiafulvalene (DM-EDT-TTF). *J. Am. Chem. Soc.* **2013**, *135*, 17176−17186.
(61) Pop, F.; Auban-Senzier, P.; Canadell, E.; Rikken, G. L. J. A.; Avarvari, N. Electrical Magnetochiral Anisotropy in a Bulk Chiral Molecular Conductor. *Nat. Commun.* **2014**, *5*, 3757.

DOI: 10.1021/acs.jpcc.7b02678
J. Phys. Chem. C 2017, 121, 12921−12927